

Universitat de Lleida

Document downloaded from:

<http://hdl.handle.net/10459.1/70465>

The final publication is available at:

[https://doi.org/10.1016/S1002-0160\(10\)60060-4](https://doi.org/10.1016/S1002-0160(10)60060-4)

Copyright

(c) Soil Science Society of China. Published by Elsevier, 2010

2
3 **Aggregate Development and Organic Matter Storage in Mediterranean**
4 **Mountain Soils**

5
6 R. M. POCH^{1,2,*2} and M. ANTÚNEZ ¹

7 ¹Department of Environment and Soil Science, University of Lleida. Av. Rovira Roure
8 191, 25198 Lleida, Catalonia
9 (Spain)

10 ²Centre Tecnològic Forestal de Catalunya, Pujada del Seminari s/n, 25280 Solsona,
11 Catalonia (Spain)

12
13 **ABSTRACT**

14 Soil aggregation and organic matter of seven soils from the pre-Pyrenean range in
15 Catalonia (NE Spain) were studied, in order to assess their quality as carbon sinks and
16 also to select the best soil management practices to preserve their quality. The soils are
17 classified as Calciustepts, Ustifluvents, Ustorhents, and Calciudolls. Main analyses were
18 for aggregate stability, organic carbon and micromorphology.

19 The highest amount of organic carbon is found in alluvial, deep soils (228 Mg C ha⁻¹),
20 and the lowest is in a shallow, stony soil with a low plant cover (78 Mg C ha⁻¹).
21 Subsurface horizons of degraded soils under pastures are the ones with smaller and
22 less-stable aggregates. In general, the intrapedal textural porosity is not affected upon
23 disruption after fast wetting. Fresh residues of organic matter (OM) are found mostly in
24 interaggregate spaces. Within the aggregates there are some organic remains that are
25 beginning to decompose, and also impregnative nodules of amorphous OM. Although
26 OM is evenly distributed among the aggregate fractions, the larger blocky peds have
27 more specific surface, contain less decomposed OM and have a lower organic/mineral
28 interphase than smaller crumb aggregates, which in turn are more stable. Soil carbon
29 storage is affected primarily by the OM inputs in the surface horizons. The mechanisms
30 favouring structuration through biological activity, creating small aggregates with
31 intrapedal stable microporosities will be the most effective to store organic carbon over
32 the mid and long term period.

33
34 *Key Words:* aggregate stability, Catalonia, soil carbon storage, soil organic matter

35
36 **INTRODUCTION**

37 Mineralization and organic matter (OM) oxidation are the main causes of carbon (C)
38 loss to the atmosphere due to anthropic activities. Mineralization is favoured by a change
39 from rangeland to agricultural uses, exposing soils to the surface, breaking aggregates
40 and making OM available for microbial activity and atmospheric agents (Batjes and
41 Bridges, 1992). These processes imply porosity changes, aggregate size variations and

42 alteration of energy and matter fluxes (Izaurrealde and Cerri, 2002), which result in the
43 conversion of C to CO₂ (Reicoski and Lindstrom, 1993), and nutrient release from
44 organic matter.

45 Among OM components, particulate organic matter (POM) includes any organic
46 fragment with a recognizable structure > 53 μm. It is often considered the active pool with
47 relatively fast turnover times (<10 years, Krull *et al.*, 2004). It represents a fraction that
48 decomposes and releases microbial exudates that promote the formation of
49 microaggregates (Six *et al.*, 2000a, 2000b). It is not only the location of OM but the
50 accessibility to decomposing microorganisms that affects the stability of organic carbon
51 (OC) in the soil. Kooistra and van Noordwijk (1995) stress the importance of the
52 heterogeneity of organic matter distribution of the soil at different observational scales,
53 and for this purpose, micromorphological analyses are especially useful. Optical
54 polarizing microscopy uses morphological criteria and degree of decomposition (Stoops,
55 2003), which can be used to classify functional groups with relevance in OM dynamics
56 (Blazejewski *et al.*, 2005). The relation between microstructure, OM and
57 (micro)biological activity has been studied by optical microscopy (Letey 1991, Brussaer
58 and Kooistra 1993, Brock 1987), and has been applied in the improvement of
59 contaminated soils (Adesodun *et al.*, 2008), management of pastures and forests
60 (Davidson *et al.*, 2002, 2004; Kodesova *et al.*, 2007) or effects of soil management
61 (Bonel *et al.*, 2005; Kapur *et al.*, 2007).

62 The objective of this study is to assess the physical protection of organic carbon
63 stocks within soil macroaggregates, their influence on soil porosity and relation with soil
64 organic carbon content, by comparing several soils along an altitudinal gradient in a
65 mountain area that is subjected to land use changes through agriculture abandonment. We
66 use a micromorphological approach that allows us to observe the spatial relationships
67 between soil organic and mineral components within the structural units.

68 69 MATERIALS AND METHODS

70 *The physical environment*

71 The study area is located in the Ribera Salada watershed in Catalonia (NE Iberian
72 Peninsula) belonging to the tributary network of the Ebro river and situated in the
73 southern part of the Pyrenean mountain range. The relief is tabular with slopes often
74 higher than 20 %. The substrate consists of massive conglomerates, calcareous
75 sandstones and siltstones. Soils are shallow, calcareous and stony. A description of the
76 complete soil survey can be found in Orozco *et al.* (2006). The predominant land use is
77 forestry, from brook forest to subalpine and submediterranean vegetation. The
78 agricultural zone is mainly planted with potatoes, alfalfa and cereals with a low level of
79 nitrogen fertilization. There are also high mountain grasslands with low levels of
80 trampling. The climate is mainly Mediterranean and varies to subalpine in the highest
81 parts of the basin.

82 83 *Experimental plots*

84 Seven experimental plots from the pre-pyrenean range in Catalonia (NE Spain) were
85 selected covering altitudinal (760 to 1420 m) and land use (pasture, forest) ranges. The

86 pastures were established during the 1950's after abandonment of agriculture. The soils
 87 are classified as Typic and Lithic Calcustepts, Ustifluvents, Ustorthents, Haplustepts
 88 and Calcudolls (SSS 2006, Table I).

89

90 TABLE I

91 Soil and land use of the plots located in the Ribera Salada catchment.

Station	Altitude m	Soil use	Soils (SSS 2006)
Torra	800	<i>Quercus ilex</i> forest	Typic Calcustepts
Canalda	760	Brook forest	Typic Ustifluvents
Cogulers shady Cogulers sunny	860	<i>Pinus sylvestris</i> forest	Typic Ustorthents Typic Calcustepts
Prat	1138	Pasture	Typic Haplustepts
Cal Ramonet pasture Cal Ramonet forest	1420	Mountain pasture <i>Pinus uncinata</i> forest	Typic Calcudolls

92

93 *Soil sampling and characterization*

94 Surface and subsurface horizons of the soils were described following SINEDARES
 95 (CBDSA, 1983) and sampled for morphological, physical, chemical, mineralogical and
 96 micromorphological analyses. Part of the bulk sample was sieved to obtain the fine earth.
 97 The rest was passed through a set of sieves to obtain four fractions (1--2 mm, 2--4 mm,
 98 4--8 mm, >8 mm) corresponding to macroaggregate classes for organic matter and
 99 micromorphological analyses. This sieving was carried out with air-dry samples with a
 100 minimal disturbance of the natural aggregates, in order to obtain the fractions that were
 101 more similar to those obtained when assessing structure in the field. The
 102 physico-chemical analyses of fifteen samples were done according to Porta *et al.* (1986),
 103 MAPA (1993) and Page *et al.* (1982). Particle-size distribution was determined by the
 104 pipette method, after organic matter removal with H₂O₂ and dispersion with
 105 Na-hexametaphosphate. Cation-exchange capacity was determined by displacement with
 106 1M NH₄OAc (pH 7) and the exchangeable cations measured by atomic absorption. Bulk
 107 density was measured in the field by the hole method (Nacci *et al.*, 1999), in order to
 108 obtain estimations of the carbon stored in the profiles.

109 Total carbon and total nitrogen were analyzed by the dry combustion Dumas method,
 110 with a TRUSPEC CN (LECO) elemental analyser. We analyzed the bulk samples and the
 111 four aggregate fractions (1--2 mm, 2--4 mm, 4--8 mm and >8mm) that were retained by
 112 dry sieving. Organic carbon was determined by the same method after removal of
 113 carbonates by HCl fumigation (Harris *et al.*, 2001). Organic carbon was also analyzed by
 114 the Walkley-Black method (Porta *et al.*, 1986).

115

116 *Structural stability methods*

117 We determined the structural stability of the aggregates <2 mm, of eleven samples by
 118 two methods: Le Bissonnais, modified by Amézketa *et al.* (1996) and the HEMC method

119 (Pierson and Mulla, 1989). The first one consists of measuring the mean diameter after
120 fast (*FWD*) and slow (*SWD*) wetting of microaggregates. For each treatment, the mean
121 weighted diameter is calculated. From these two values, an index of aggregate stability
122 ($AS = FWD/SWD$) was derived, in such a way that stable aggregates will yield values near
123 1.

124 The HEMC method (Pierson and Mulla, 1989; Levy and Mamedov, 2002) measures
125 the changes of the sizes of interaggregate pores when they are subjected to fast wetting
126 compared to slow wetting. In this method, the wetting process of the aggregates is
127 accurately controlled, and the energy of hydration and entrapped air are the only forces
128 responsible for aggregation breakdown. It consists of measuring the water retention
129 curves (High-Energy-Moisture-Characteristic curves, HEMC) of the aggregates in a
130 suction funnel with a porous ceramic plate, at high matric potentials. The saturated
131 sample is subjected to desorption from 0 and 20 hPa pressure heads, at intervals of 2 cm.
132 The experimental values were adjusted to a Log-Normal curve (Kosugi, 1996) using the
133 RETC 6.0 software (Van Genuchten *et al.*, 1991). Two HEMC are obtained per sample,
134 by two different pre-treatments: the first one is slowly wetted by capillarity, the second
135 one is submerged in a water layer deep enough to just cover all the aggregates (fast
136 wetting). From each curve, a structural index is calculated:

$$137 \quad \text{Structural Index}(SI) = \frac{\text{drained pore volume}}{|\text{modal matric potential}|}$$

138 The drained pore volume is defined from the water capacity curve ($d\theta/d\psi$), as the
139 area below the curve and above its baseline. The latter represents the rate of water loss
140 due to aggregate shrinkage rather than pore emptying (Collis-George & Figueroa, 1984;
141 Levy and Mamedov, 2002). The modal potential is the maximum value of the water
142 capacity curve, θ being the water content (kg kg^{-1}) and ψ the matric potential (cm). As
143 aggregate slake and the pore sizes distribution changes, the modal suction increases and
144 the volume of drainable pores decrease. These changes cause the value of the structural
145 index decreases (Pierson & Mulla, 1989). The stability index S is calculated as: $S = SI$
146 (*fast wetting*)/ SI (*slow wetting*). A high stability will yield values near unity, indicating
147 that a fast wetting does not change pore characteristics. A collapse of aggregates after fast
148 wetting, on the contrary, will mean a change of pore volume or diameter, normally lower,
149 which results in a S value near 0.

150

151 *Micromorphology and image analyses*

152 Vertical thin sections, 13 cm long, 5.5 cm wide, were made from air-dried
153 undisturbed soil blocks of seven horizons, according to the methods described in Murphy
154 (1986). Because of their nature, no special drying methods were required in order to
155 maintain their original structure. They were studied with the petrographic microscope
156 (Olympus BX51) following the guidelines of Stoops (2003), mainly at magnifications of
157 2x and 4x but also 10x for special pedofeatures. Thin sections were also made of four
158 aggregate fractions of each sample: 1--2 mm, 2--4 mm, 4--8 mm and >8 mm. Image
159 analyses were performed with ImageJ, a public domain Java image processing program
160 (Rasband, 2008).

161

162 *Porosity measurements*

163 Ten fields for undisturbed samples and five fields for each aggregate class were
164 randomly selected from the respective thin sections. Two images were taken from each
165 field with the petrographic microscope, under parallel polarized light (PPL) and under
166 partly crossed polarizers (PXPL). The sizes of the images were 6.1 x 4.4 mm for the
167 undisturbed samples and 1.2 x 0.88 mm for the aggregates. The PXPL image was edited
168 and binarized by an upper and lower threshold that selected the gray levels corresponding
169 to the pore space, disregarding the brightest (quartz grains) and darkest (organic particles
170 and opaques) particles. The PPL image was used as control to remove the solid particles
171 with gray levels similar to the pores and artifacts such as air bubbles. Outliers were
172 removed and only the objects larger than 20 μm (undisturbed samples) and 4 μm
173 (aggregate samples) were retained for measurements, which corresponds to the minimum
174 equivalent diameter of the pores that have been measured by the image analyser software
175 (ImageJ, Rasband, 2008). From each image, field parameters (area percentage, perimeter
176 and number of objects) and object parameters (size, perimeter, circularity defined as 4π
177 $\text{area} \cdot \text{perimeter}^{-2}$ and feret diameters) were obtained.

178

179 *Particulate organic matter*

180 Images of particulate organic matter (POM) larger than 4 μm contained in each
181 aggregate class were obtained from the petrographic microscope with vertical incident
182 light (IL), in the same fields as the porosity measurements. The process of image editing
183 was similar to that of the porosity, except for the threshold which selected only the
184 darkest spots. PPL images of the same field were used as visual control to remove
185 artifacts. Opaque elements as iron oxides did not interfere, because the soils did not show
186 redoximorphic features. Also, the baseline of opaque minerals was low and constant
187 through all the sites, since the lithology of the parent material is calcareous, contains low
188 amounts of opaques and is very homogeneous. Besides, the minerals had a reflection
189 behaviour different from the OM. The same field and object parameters as for porosity
190 were calculated for POM.

191

192 *Statistical methods*

193 Statistical analysis was performed with the PAST v. 1.53 programme (Hammer *et al.*,
194 2001). F and t tests were used for mean separation. Linear regressions were used for
195 comparisons between methods. ANOVA was used with Tukey's test for pairwise
196 comparisons.

197

198 **RESULTS**

199 *Organic matter storage*

200 The soils are sandy loam, calcareous and with carbon contents (LECO method)
201 between 0.13 and 0.65 g kg^{-1} (Table II).

202

203

204 TABLE II

205 Soil characteristics and soil carbon storage

Soil	Depth	Horizon	Texture	pH	CaCO ₃ eq.	Organic Carbon (Walkley-Black)	Organic Carbon (LECO)	Nitrogen	C/N	Bulk Density	Carbon storage **	Land use
	cm				g kg ⁻¹	g kg ⁻¹	g kg ⁻¹	g kg ⁻¹		kg m ⁻³	Mg C ha ⁻¹	
Canalda	0--14	A	L-SL	7.7	2.147	0.636	0.646	0.0494	16.8	1210	228	Riparian forest
	14--34	Bw	L-SL	8.3	3.128	0.188	0.491	0.0182	18.0			
Cogulers shady	0--17	A	L	7.8	1.905	0.260	0.482	0.0285	15.5	1130	192	Pine forest
	17--35	Bw	SL	8.2	2.066	0.274	0.489	0.0245	14.3			
Torra	0--13	A	SL	7.4	0.009	0.212	0.341	0.0205	13.4	1270	85	Oak forest
	13--30	Bw	SL	8.3	0.035	0.089	0.131	0.0148	8.8			
Prat	0--15	A	SL	7.7	0.045	0.291	0.421	0.0393	23.4	1360	164	Pasture
	15--30	Bw1	SL	8.3	0.064	0.145	0.195	0.0182	7.6			
	30--42	Bw2		8.6	0.051	0.177	0.235	0.0440	8.2			
Cogulers sunny	0--17	A	SL	8.6	3.129	0.157	0.362	0.0206	9.6	1270	166	Pine forest
	17--30	Bwk	L	8.3	3.133	0.307	0.533	0.0374	14.4			
Cal Ramonet Forest	0--12	A	SL	7.5	0.154	0.259	0.216	0.0316	16.7	1220	110	Pine forest
	12--40	AB		8.2	0.132	0.141	0.230	0.0144	13.8			
Cal Ramonet Pasture	0--10	Ap	SL	8	0.331	0.189	0.359	0.0299	9.5	1150	78	Pasture
	10--20	Ap		8.2	0.397	0.164	0.317	0.0240	10.1			

206 Both OC determinations are positively correlated ($R^{**}=0.55$), according to the
207 following linear regression: $OC_{LECO} = 1.410 OC_{W-B}$. This relation indicates that not all the
208 organic carbon is oxidized by the Walkley-Black method, or that there are other sources
209 of carbon, as charcoal from pasture burning, that are not adequately quantified by these
210 methods. Subsurface horizons sometimes have higher C content than surface horizons,
211 due to the fluventic character and to mass movements along steep slopes. C/N ratios
212 indicate a mull or moder humus type, due to the presence of conifers and grasses. The
213 highest amount of organic carbon stored (228 Mg ha^{-1}) is found in alluvial soils. The
214 lowest (78 and 85 Mg ha^{-1}) correspond to stony soils with low plant cover and
215 overgrazed.

216 Organic carbon content in each macroaggregate class of surface and subsurface
217 horizons is found in Fig. 1.

218

219 Fig. 1. Organic carbon content of macroaggregates grouped according to type of horizon.
220 Bars indicate half of the standard deviation ($n=5$ surface horizons, $n=6$ subsurface
221 horizons). Values of the aggregate classes are compared within each group (letters a,b,
222 $P<0.10$) and between groups (letters x,y*). Average values followed with the same letter
223 are not significantly different.

224

225 When treated as a whole there are no significant differences of OC content, but
226 within the surface horizons, the largest macroaggregates (4--8 mm) have less OC than the
227 rest. Besides, the aggregates < 4 mm have significantly more OC in the surface than in the
228 subsurface horizons. No differences are observed when grouped according to type of
229 vegetation or land use.

230 *Aggregate stability*

231 The values of the two stability indices for aggregates < 2 mm are plotted in Fig. 2,
232 grouped according to the type of horizon (surface / subsurface).

233

234 Fig. 2. Structural stability indices of the studied horizons for aggregates < 2 mm:
235 Stability index S (Pierson and Mulla, 1989) and Aggregate Stability index AS (from
236 Amézketa *et al.*, 1996), grouped according to the type of horizon: surface (left) and
237 subsurface (right). Values are the average of 2 replications.

238

239 Neither sample depth nor land use affect aggregate stability. Walkley-Black organic
240 carbon content is positively correlated with $R = 0.69$ ($P<0.05$) with the stability of
241 aggregates estimated with the method of Amézketa *et al.* (1996), and negatively
242 correlated ($R = -0.60$, $P<0.10$) with the structural index of Pierson and Mulla (1989). It
243 suggests that a higher OC content maintains the size of the aggregates after a fast wetting,
244 but diminishes the volume and/or the size of the pores within them.

245

246 *Porosity, aggregation and organic residues*

247 The undisturbed soil samples of three A and four Bw horizons show a strong
248 aggregation, either as rounded (crumb) aggregates (Fig. 3) or subangular blocks.

249

250 Fig. 3. Microphotograph of horizon A, Cal Ramonet Forest. Fresh root residues (RR)
251 between peds and amorphous organic matter (AOM) within peds. Image length 6.1 mm.
252 PPL.

253

254 The latter predominate in B horizons, although mixed (compound) microstructures
255 are often found. Table III shows the main micromorphological characteristics of the
256 samples regarding porosity, aggregation and organic matter.

257 TABLE III
258 Micromorphological characteristics of the soils

Soil	Depth cm	Horizon	Microstructure	Porosity	c/f ratio and related distribution	Coarse elements	Organic components
	cm			(%)			
Cal Ramonet Forest	0--10	A	Highly separated crumb, css.	Complex packing voids; fissures, moderately accommodated, horizontal (50)	1/3 Double space porphyric	Medium sand, quartz	Very frequent root and leaf sections, fresh and slightly decomposed between peds, more decomposed within peds; organic pigment and punctuations.
Cogulers sunny Cogulers shady	0--10	A	Highly separated granular, fss and vfss.	Complex packing voids, biopores (50)	1/1 Close porphyric	Coarse sand of calcareous sandstone, fine and very fine sand of quartz and sparite	Frequent root and leaf sections, fresh and slightly decomposed, some of them phlobaphenized; very abundant organic pigment and punctuations.
	0--15	A	Moderately separated subangular blocky vcss and css, juxtaposed with granular vfss due to faunal activity.	Complex packing voids; fissures, moderately accommodated (50)	2/1 Close porphyric	Coarse and very coarse sand of quartz and sparite, Sand and gravels of quartzitic sandstone	Frequent root and leaf sections, fresh and slightly decomposed between peds, more decomposed within peds; frequent physical decomposition by faunal activity; organic amorphous residues; organic pigment and punctuations.
Prat	15--30	Bw	Moderately separated subangular blocky vcss and css.	Planar voids, partly accommodated; intrapedal vughs and chambers, css (55)	2/1 Close porphyric	Very coarse sand of quartz, quartzites and calcareous sandstone. Very fine sand of quartz and sparite.	Root sections, fine, slightly decomposed, some of them phlobaphenized. Organic pigment and punctuations.
	13--28	Bw1	Highly separated granular, bimodal distribution of peds: mss and fss	Complex packing voids (60)	3/1 Close porphyric	Medium sand of quartzite and quartz.	Black amorphous residues, vfss, intra and interaggregate.
	28--40	Bw2	Moderately separated subangular blocky, mss.	Fissures and chambers, partly filled with smaller rounded aggregates. Complex packing voids (50)	2/1 Close porphyric	Medium sand of quartzite and quartz.	Few root sections and plant residues. Frequent organic pigment and amorphous organic matter and punctuations, irregularly distributed in peds. Abundant faunal activity, mixing soil materials.
Torra	13--30	Bw	Moderately separated subangular blocky, mss	Fissures, moderately accommodated; and chambers (35)	3/1 Close porphyric	Very coarse sand and gravels of calcarous sandstone; medium sand of quartz and quartzite.	Organic pigment; root sections and tissue remains, moderately decomposed between peds, highly decomposed within peds.

259 Vcss: very coarse sand size; css: coarse sand size; mss: medium sand size; fss: fine sand size; vfss: very fine sand size

260 The high aggregate separation is due to moderately accommodated planar voids
261 between blocks, but also to compound and complex packing voids between rounded
262 aggregates and/or sands and gravels. Organic matter is mainly found as fresh root
263 sections and leaf residues between peds, which become moderately decomposed when
264 found within the peds (Fig. 3). In the same horizons there is evidence of the mixture of
265 amorphous organic matter, mostly by faunal activity, which originates aggregates with
266 heterogeneous distribution of organic matter content, and allows one to find all gradations
267 of organic matter, from plant residues and cells to organic pigment. The latter is found
268 either concentrated as moderately impregnative orthic nodules, or uniformly mixed in the
269 micromass.

270 The edition and binarization of these images allows the quantification of the porosity,
271 which is shown in Table IV.

272 TABLE IV.

273 Image analyses of pores > 20 µm (equivalent diameter) on undisturbed samples. Values without letters or followed by the same letter are not
 274 significantly different within a column ($P < 0.05$, $n=10$).

275

Soil	Depth	Horizon	Field parameters			Pore parameters		
			Total porosity	Total perimeter	Number	Area	Perimeter	Circularity
	cm		%	mm mm ⁻²	count mm ⁻²	mm ²	mm	
Cal Ramonet	0--10	A	29.22 bc	5.70 b	10.89	0.0289 ab	0.506	0.7356 ab
Forest								
Cogulers sunny	0--10	A	25.27 b	4.56 ab	9.72	0.0471 a	0.631	0.5711 a
Cogulers shady	0--15	A	24.48 b	4.94 ab	17.42	0.0169 b	0.312	0.7194 ab
	15--30	Bw	22.84 b	4.93 ab	16.19	0.0197 ab	0.362	0.7563 b
Prat	13--28	Bw1	36.76 c	5.95 b	10.46	0.0394 ab	0.593	0.7559 b
	28--40	Bw2	22.60 b	6.18 b	15.94	0.0144 b	0.403	0.7190 ab
Torra	13--30	Bw	10.34 a	3.18 a	13.31	0.0109 b	0.295	0.7471 b

276

277 Fig. 4 displays the boxplots of the image variables showing significant differences
278 between samples. The less porous sample is the Bw horizon of Torra, a degraded soil
279 under an oak forest with a subangular blocky structure. This horizon also has the lowest
280 specific surface, indicated by a low total perimeter. The most porous horizon is the upper
281 Bw of the pasture soil of Prat. It has a very well developed crumb structure with large
282 packing pores in between. The largest and more circular pores are found in the A horizon
283 of Cogulers sunny under forest, which correspond to equant packing voids (connected
284 pores due to packing of equidimensional particles, Stoops, 2003) and biopores due to a
285 high faunal activity.

286

287 Fig. 4. Boxplots of total area, total perimeter, pore area and pore circularity of six
288 horizons. Solid lines in boxes indicate median values. Boxes show the 25--75 % quartiles.
289 Whisker caps indicate the minimal and maximal values (n=10). Boxes followed with the
290 same letter are not significantly different*. RForA: Ramonet Forest, A horizon; CSuA:
291 Cogulers Sunny, A horizon; CShA: Cogulers Shady, A horizon; CShBw: Cogulers
292 Shady, Bw horizon; PBw1: Prat, Bw1 horizon; PBw2: Prat, Bw2 horizon; TBw: Torra,
293 Bw horizon.

294

295 Table V and Fig. 5 show some of the parameters of image analyses of the porosity
296 and particulate organic matter of the aggregates.

297

298 Fig. 5. Boxplots of pore parameters and particulate organic matter (POM) of aggregates.
299 Solid lines in boxes indicate median values. Boxes show the 25--75 % quartiles. Whisker
300 caps indicate the minimal and maximal values (n=8). Boxes followed with the same letter
301 are not significantly different ($P < 0.10$).

302 TABLE V

303 Summary of the image analyses of pores and organic matter (> 4 μm equivalent diameter) in aggregates. Values without letters or followed by the
 304 same letter are not significantly different within a column ($P < 0.10$, $n=8$).

305

Aggregate class	Porosity					Organic matter				
	Total porosity	Total perimeter	Number	Pore area	Pore circularity	Total area	Total perimeter	Number	Object Area	Object Circularity
	%	mm mm ⁻²	count mm ⁻²	mm ²		%	mm mm ⁻²	count mm ⁻²	mm ²	
1--2 mm	8.67	9.49 a	97.3	0.00256	0.64	1.62 a	6.16 a	102.7 a	0.000234	0.69
2--4 mm	7.96	8.94 a	98.5	0.00220	0.66	1.85 a	3.98 bc	84.6 a	0.000250	0.76
4--8 mm	10.73	9.78 a	102.3	0.00136	0.66	1.10 b	2.68 b	58.6 b	0.000197	0.70
> 8 mm	14.07	15.79 b	180.4	0.00112	0.68	1.78 a	4.73 ac	100.8 a	0.000237	0.73

306

307 No differences between horizon type nor position have been found, but for some
308 properties there are differences between aggregate classes: large aggregates tend to be
309 more porous and have more specific surface than smaller ones (significance level of
310 10 %). The specific surface of POM increases in the three smaller aggregate classes. This
311 means a higher interphase of POM with mineral material as the aggregate size diminishes.
312 A high degree of digitation of the particles could be the reason for this behaviour, as it is
313 observed in thin sections.

314

315 DISCUSSION AND CONCLUSIONS

316 The structure of these soils is characterized by large macroaggregates with high porosities,
317 but this porosity is probably not very stable. Kay (1997) indicates that the macropores are
318 unstable unless the process of creating the pore does not substantially increase the OC
319 content of the pore wall, as it happens with root channels or some faunal pores. In our
320 case the smallest macroaggregates are less porous, have less specific surface and contain
321 more OM than the larger ones. This is in agreement with the observations of Jastrow and
322 Miller (1997) and Angers and Chenu (1997).

323 The analyses of the stability indices of the aggregates < 2 mm and the microscopical
324 observations suggest that the process of aggregate breakdown is controlled by fissuration
325 of large pedis (crumbs or subangular blocks), which does not mean a collapse of
326 intrapedal packing voids or biopores, which remain in smaller aggregates. Organic matter
327 evolution observed in undisturbed blocks results in morphologies from fresh plant
328 remains to amorphous organic masses with diffuse boundaries, that break down and
329 become incorporated within the mineral material mostly by biological activity. Thus, it
330 would be the OM decomposition rates that control the formation and stabilization of
331 microaggregates, as observed by Jastrow and Miller (1997), rather than the mere presence
332 of organic structures such as roots or hyphae. The higher decomposition degree in the
333 smaller aggregates is shown by a higher organic/mineral interphase, that corresponds to a
334 process of progressive matrix impregnation by the remaining OM in the form of
335 amorphous impregnative nodules, sometimes digitated, that probably provide the
336 aggregates with a higher stability. In a system with a regular supply of organic matter
337 residues such as roots or litter, the cycle of organic matter turnover would evolve from
338 fresh organic remains to occluded organic carbon in the smallest aggregates, in agreement
339 with the model of Six *et al.* (2000a). Initially, macroaggregates are formed around fresh
340 residues, namely coarse intraaggregate particulate organic matter (iPOM), since these
341 residues promote microbial activity that produces cohesive compounds (Golchin *et al.*,
342 1994; Jastrow, 1996; Six *et al.*, 1999), and are a source of organic C. Our
343 micromorphological observations (shape and amount of POM in aggregates) are in
344 agreement with the analytical ones of Fonte *et al.* (2010), who stress the importance of
345 POM in the stability of large macroaggregates under forest. Similarly, Huang *et al.* (2010)
346 show that OM supply promotes the formation of microaggregates within
347 macroaggregates, leading to more stabilization of new POM.

348 The results provide micromorphological evidence for the importance of OM supply
349 in forest and range environments: soils with organic inputs tend to form stable aggregates,
350 which in turn can protect soil OM (SOM) from decomposition, leading to further

351 aggregate stabilization. This is in agreement with Álvaro-Fuentes *et al.* (2009),
352 Fernández-Ugalde *et al.* (2009) and Xi *et al.* (2010), who found that no tillage promoted
353 OM accumulation in microaggregates and a better structure. However, in soils degraded
354 by erosion or compaction, the disruption of aggregates exposes previously protected OM
355 to decomposing agents, leading to a greater loss of SOM and a further destabilization of
356 aggregates (Jastrow and Miller, 1997). In our case, organic matter storage seem more
357 effective in small aggregates of surface horizons: they are more stable and contain more
358 carbon than larger aggregates. They correspond to crumbs smaller than 1 mm (Table III).

359 Any physical disturbance on forest soils (logging, rainfall, erosion) may break down
360 aggregates, which implies OM losses; but despite this loss, the remaining smaller
361 aggregates, if the system is not excessively degraded, are the ones that may store OC in a
362 more effective way.

363

364

365 REFERENCES

366 Adesodun, J. K., Davidson, D. A. and Mbagwu, J. S. C. 2008. Soil faunal activity of an
367 oil-polluted tropical alfisol amended with organic wastes as determined by
368 micromorphological observations. *Applied Soil Ecology*. **39**: 46--57.

369

370 Álvaro-Fuentes, J., Cantero-Martínez, C., López, M. V., Paustian, K., Deneff, K., Stewart,
371 C. E. and Arrúe, J. L. 2009. Soil aggregation and soil organic carbon stabilization: Effects
372 of management in semiarid Mediterranean agroecosystems. *Soil Science Society of
373 America Journal*. **73**: 1519--1529.

374

375 Amézketa, E., Singer, M. J. and Le Bissonnais, Y. 1996. Testing a new procedure for
376 measuring water-stable aggregation. *Soil Science Society of America Journal*. **60**:
377 888--894.

378

379 Angers, D. A. and Chenu, C. 1997. Dynamics of soil aggregation and C sequestration. *In*
380 Lal, R., Kimble, J.M., Follett, R.F. and Stewart, B.A. (eds.) *Soil Processes and the
381 Carbon Cycle*. CRC Press, Boca Raton, USA. pp. 199--208.

382

383 Batjes, N. H. and Bridges, E. M. 1992. A review of soil factors and processes that control
384 fluxes of heat, moisture and greenhouse gases. Technical Paper 23, International Soil
385 Reference and Information Centre (ISRIC), Wageningen, The Netherlands. 201 pp.

386

387 Blazejewski, G. A., Stolt, M. H., Gold, A. J. and Groffman, P. M. 2005. Macro- and
388 micromorphology of subsurface carbon in riparian zone soils. *Soil Science Society of
389 America Journal*. **69**: 1320--1329.

390

391 Bonel, B. A., Morrás, H. J. M. and Bisaro, V. 2005. Modificaciones de la microestructura
392 y la materia orgánica en un argiudol bajo distintas condiciones de cultivo y conservación.
393 *Ciencia del Suelo*. **23**: 1--12.

394

395 Brock, T. D. 1987. The study of the microorganisms in situ: Progress and problems. *In*
396 Fletcher, M., Gray, T.R.G. and Jones, J.G. (eds.) *Ecology of microbial communities*.
397 Society of General Microbiology. Cambridge, UK. pp 1--17.

398

399 Brussaar, L. and Kooistra, M. J. (eds.) 1993. Soil structure/Soil biota interrelationships.
400 *Geoderma*. **56**. Monograph, 647 pp.

401

402 CBDSA – Comisión Banco de Datos de Suelos y Aguas. 1983. SINEDARES, Manual
403 para la descripción codificada de suelos en el campo. Ministerio de Agricultura, Pesca y
404 Alimentación de España, Madrid, Spain. 137 pp.

405

406 Collis-George, N. and Figueroa, B. S. 1984. Use of high energy moisture characteristic to
407 assess soil stability. *Australian Journal of Soil Research*. **22**: 349--356.

408
409 Davidson, D. A., Bruneau, P. M. C., Grieve, I. C. and Wilson, C. A. 2004.
410 Micromorphological assessment of the effect of liming on faunal excrement in an upland
411 grassland soil. *Applied Soil Ecology*. **26**: 169--177.
412
413 Davidson, D. A., Bruneau, P. M. C., Grieve, I. C. and Young, I. M. 2002. Impacts of fauna
414 on an upland grassland soil as determined by micromorphological analysis. *Applied Soil*
415 *Ecology*. **20**: 133--143.
416
417 Fernández-Ugalde, O., Virto, I., Bescansa, P., Imaz, M.J., Enrique, A. and Karlen, D.L.
418 2009. No-tillage improvement of soil physical quality in calcareous, degradation-prone,
419 semiarid soils. *Soil & Tillage Research*. **106**: 29--35.
420
421 Fonte, S.J., Barrios, E. and Six, J. 2010. Earthworms, soil fertility and
422 aggregate-associated soil organic matter dynamics in the Quesungual agroforestry system.
423 *Geoderma*. **155**: 320--328.
424
425 Golchin, A., Oades, J. M., Skjemstad, J. O. and Clarke, P. 1994. Soil structure and carbon
426 cycling. *Australian Journal of Soil Research*. **32**: 1043--1068.
427
428 Hammer, Ø., Harper, D.A.T. & Ryan, P.D. 2001. PAST: Palaeontological Statistics
429 software package for education and data analysis. *Palaeontologia Electronica*. **4**: 1--9.
430
431 Harris, D., Horwath, W. R. and Van Kessel, C., 2001. Acid fumigation of soils to remove
432 carbonates prior to total organic carbon or carbon-13 isotopic analysis. *Soil Science*
433 *Society of America Journal*. **65**: 1853--1856.
434
435 Huang, S., Peng, X., Huang, Q. and Zhang, W. 2010. Soil aggregation and organic carbon
436 fractions affected by long-term fertilization in a red soil of subtropical China. *Geoderma*.
437 **154**: 364--369.
438
439 Izaurrealde, R. C. and Cerri, C. C. 2002. Organic matter management. *In* Lal, R. (ed)
440 *Encyclopedia of Soil Science*. Marcel Dekker, New York, USA. pp. 910--916.
441
442 Jastrow, J. D. 1996. Soil aggregate formation and the accrual of particulate and
443 mineral-associated organic matter. *Soil Biology and Biochemistry*. **28**: 665--676.
444
445 Jastrow, J. D. and Miller, R. M. 1997. Soil aggregate stabilization and carbon
446 sequestration: Feedbacks through organo-mineral associations. *In* Lal, R., Kimble, J.M.,
447 Follett, R.F. and Stewart, B.A. (eds.) *Soil Processes and the Carbon Cycle*. CRC Press,
448 Boca Raton, USA. pp. 207--224.
449
450 Kapur, S., Ryan, J., Akça, E., Çelik, I., Pagliai, M. and Tülün, Y. 2007. Influence of
451 mediterranean cereal-based rotations on soil micromorphological characteristics.

452 *Geoderma*. **142**: 318--324.

453

454 Kay, B. D. 1997. Soil structure and organic carbon: A review. *In* Lal, R., Kimble, J.M.,
 455 Follett, R.F. and Stewart, B.A. (eds.) *Soil Processes and the Carbon Cycle*. CRC Press,
 456 Boca Raton, USA. pp. 169--198.

457

458 Kodesova, R., Pavlu, L., Kodes, V., Zigova, A. and Nikodem, A. 2007. Impact of spruce
 459 forest and grass vegetation cover on soil micromorphology and hydraulic properties of
 460 organic matter horizon. *Biologia*. **62**: 565--568.

461

462 Kooistra, M. J. and van Noordwijk, M. 1995. Soil architecture and distribution of organic
 463 matter. *In* Carter, M. R. and Stewart, B. A. (eds) *Structure and Organic Matter Storage in*
 464 *Agricultural Soils*. Lewis Publishers, Boca Raton, USA. pp. 15--56.

465

466 Kosugi, K. 1996. Lognormal distribution model for unsaturated soil hydraulic properties.
 467 *Water Resources Research*. **32**: 2697--2703.

468

469 Krull, E. S., Skjemstad, J. O. and Baldock, J. A. 2004. Functions of soil organic matter
 470 and the effect on soil properties. Grains Research and Development Corporation Report
 471 Project No. CSO 00029. Adelaide, Australia. 107 pp.

472

473 Letey, J. 1991. The study of soil structure: Science or art. *Australian Journal of Soil*
 474 *Research*. **29**: 699--707.

475

476 Levy, G. J. and Mamedov, A. I. 2002. High-energy-moisture-characteristic aggregate
 477 stability as a predictor for seal formation. *Soil Science Society of America Journal*. **66**:
 478 1603--1609.

479

480 MAPA-Ministerio de Agricultura, Pesca y Alimentación. 1993. Métodos Oficiales de
 481 Análisis. Tomo III, Ministerio de Agricultura, Pesca y Alimentación de España. Madrid,
 482 Spain. 662 pp.

483

484 Murphy, C. P., 1986. *Thin Section Preparation of Soils and Sediments*. A.B. Academic
 485 Publishers, Berkhamsted, UK. 149 pp.

486

487 Nacci, S., Poch, R. M. and Pla, I. 1999. Propiedades físicas de los suelos y diagnóstico de
 488 su degradación. *Quaderns DMACS 22*, Paperkite Editorial, Lleida, Spain. 51 pp.

489

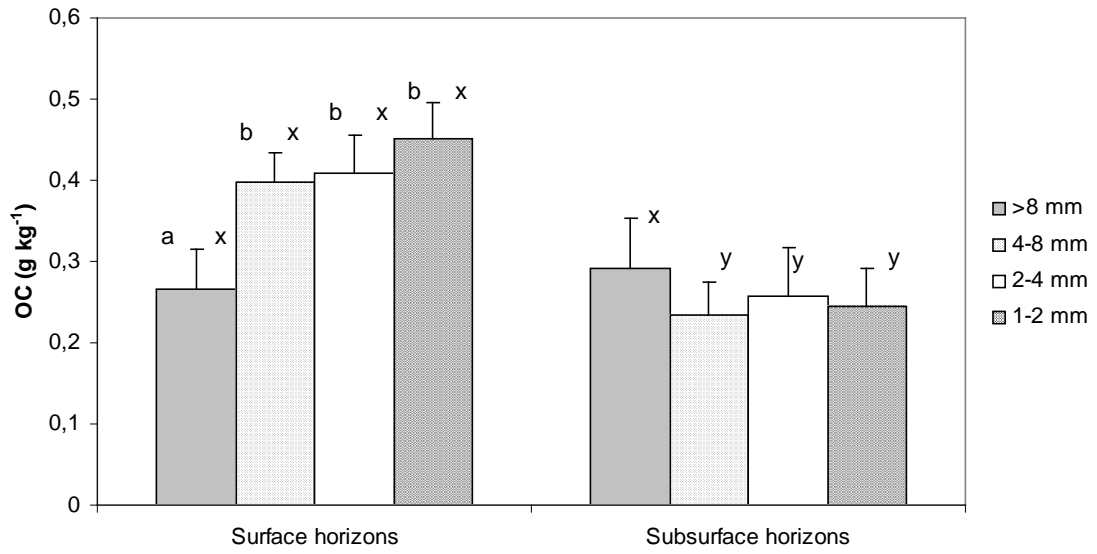
490 Orozco, M., Poch, R. M., Batalla, R. J. and Balasch, J. C. 2006. Hydrochemical budget of
 491 a Mediterranean mountain basin in relation to land use (The Ribera Salada, Catalan Pre -
 492 Pyrenees, NE Spain). *Zeitschrift für Geomorphologie*. **50**: 77 -- 94.

493

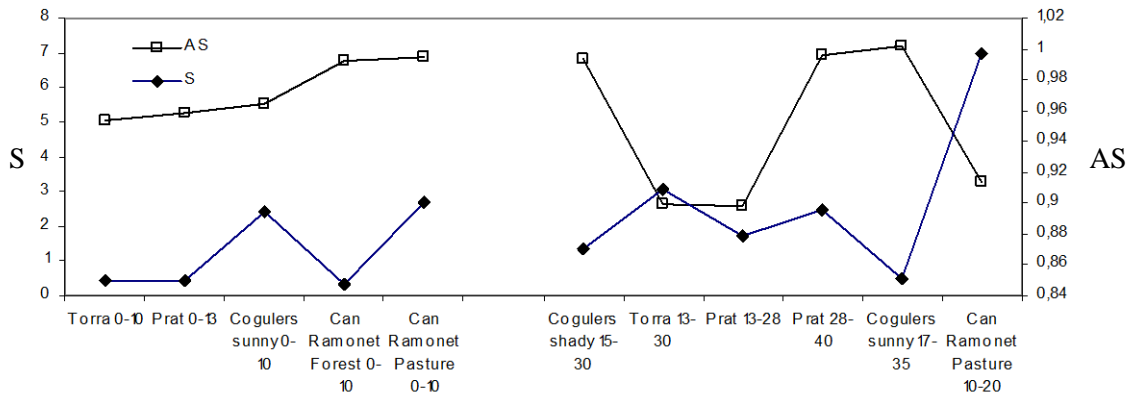
494 Page, A. L., Miller, R. H., and Keeney, D. R. (eds.) 1982. *Methods of Soil Analysis II.*
 495 *Chemical and Microbiological Properties*. (2nd Ed). ASA-SSSA, Madison, USA. 1159

496 pp.
497
498 Pierson, F. B. and Mulla, D. J. 1989. An improved method for measuring aggregate
499 stability of a weakly aggregated loessial soil. *Soil Science Society of America Journal*. **53**:
500 1825--1831.
501
502 Porta, J., López-Acevedo, M. and Rodríguez, R. 1986. Técnicas y experimentos en
503 Edafología. Col·legi Oficial d'Enginyers Agrònoms de Catalunya, Barcelona, Spain. 282
504 pp.
505
506 Rasband, W. 2008. ImageJ 1.40. National Institute of Health, USA. Available on line at
507 <http://rsb.info.nih.gov/ij/> (Verified on October 9, 2009).
508
509 Reicoski, D. C. and Lindstrom, M. J. 1993. Fall tillage method: Effect from short term
510 carbon dioxide flux from soil. *Agronomy Journal*. **85**: 1237--1243.
511
512 Six, J., Elliott, E. T. and Paustian, K. 2000a. Soil macroaggregate turnover and
513 microaggregate formation: a mechanism for C sequestration under no-tillage agriculture.
514 *Soil Biology and Biochemistry*. **32**: 2099--2103.
515
516 Six, J., Paustian, K., Elliot, E. T. and Combrink, C. 2000b. Soil structure and organic
517 matter: I. Distribution of aggregate-size classes and aggregate-associated carbon. *Soil*
518 *Science Society of America Journal*. **64**: 681--689.
519
520 Six, J., Paustian, K., Elliot, E. T. 1999. Aggregate and soil organic matter dynamics under
521 conventional and no-tillage systems. *Soil Science Society of America Journal*. **63**:
522 1350--1358.
523
524 SSS – Soil Survey Staff. 2006. Keys to Soil taxonomy. Ninth edition. SSS Soil
525 Conservation Service. Agricultural US Government Printing Office, Washington, D. C.,
526 USA. 333 pp.
527
528 Stoops, G., 2003. Guidelines for Analysis and Description of Soil and Regolith Thin
529 Sections. Soil Science Society of America, Madison, USA. 184 pp.
530
531 Van Genuchten, M. Th., Leij, F. J. and Yates, S. R. 1991. The RETC code for quantifying
532 the hydraulic functions of unsaturated soils, Version 1.0. EPA Report 600/2-91/065, US
533 Salinity Laboratory, USDA, ARS, Riverside, California, USA. 85 pp.
534
535 Xi, X.M., Li, X.G., Long, R.J., Li, Z.T. and Li, F.M. 2010. Dynamics of soil organic
536 carbon and nitrogen associated with physically separated fractions in a
537 grassland-cultivation sequence in the Qinghai-Tibetan plateau. *Biology and Fertility of*
538 *Soils*. **46**: 103--111.
539

540
541

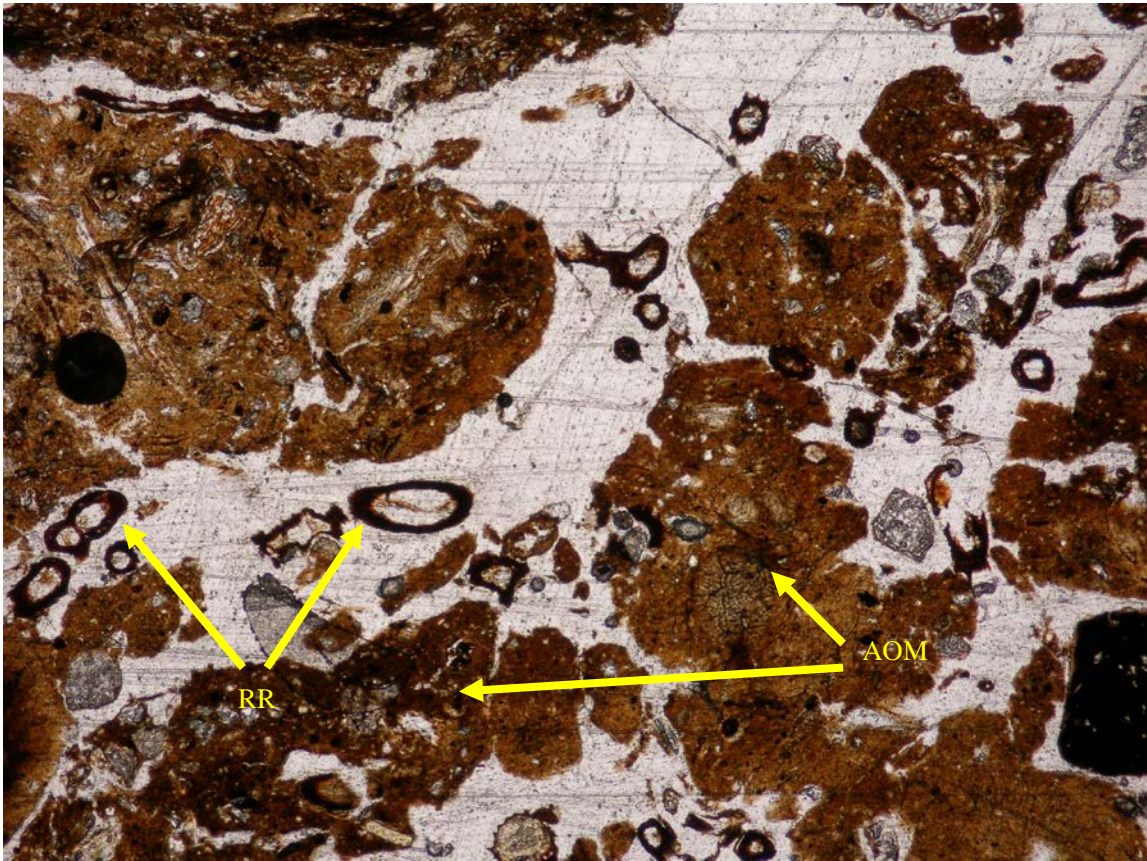


542
543 Fig 1.
544
545
546



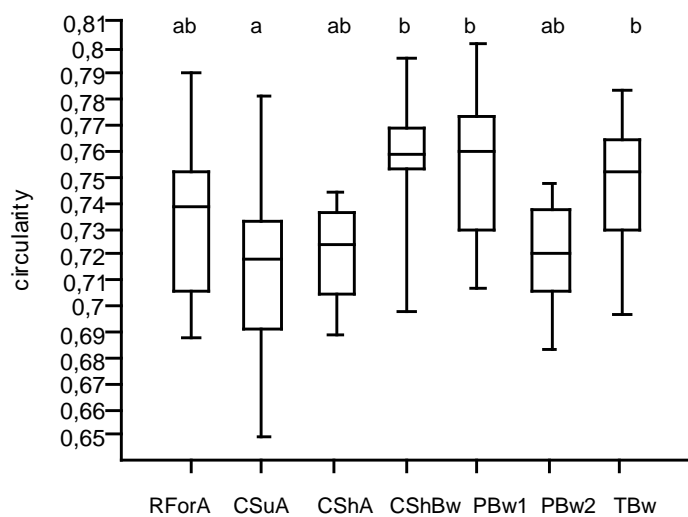
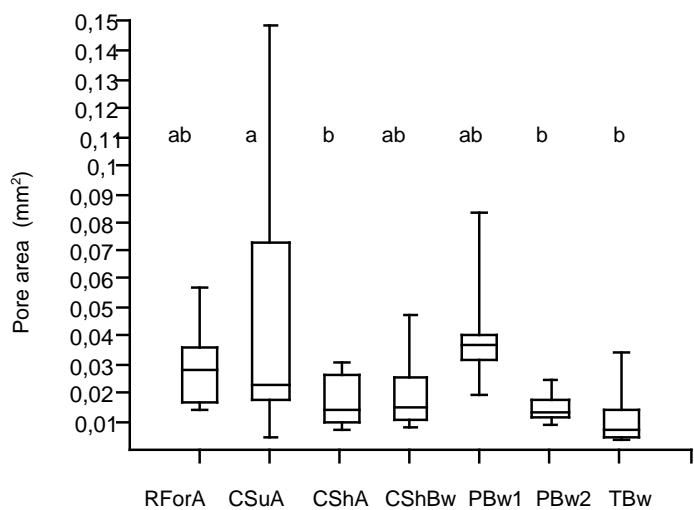
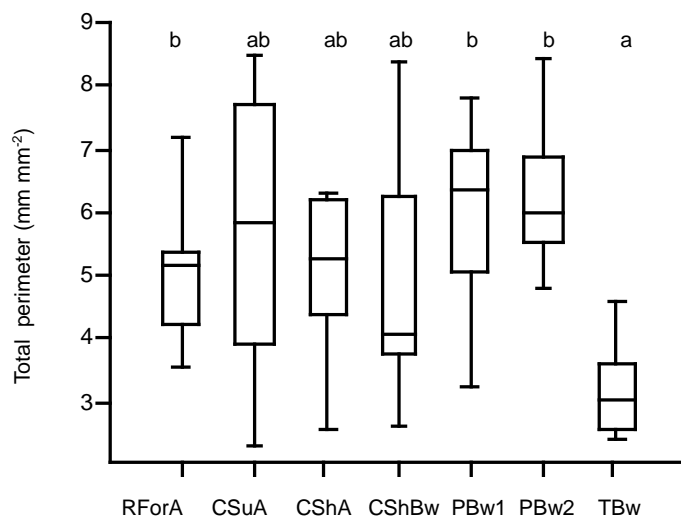
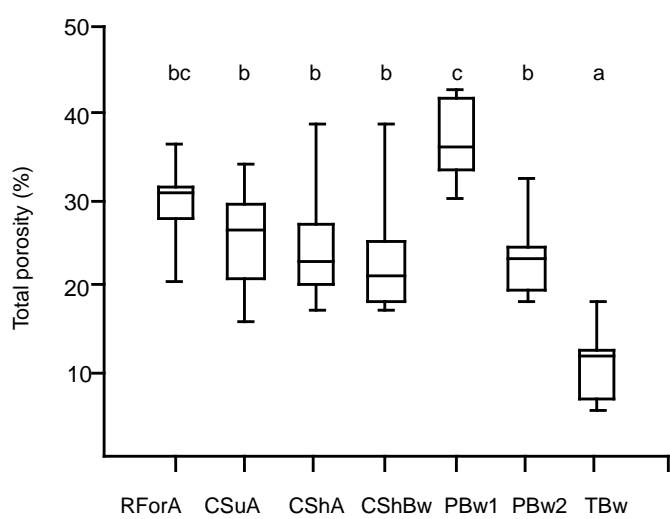
547
548 Fig. 2.
549

550
551



552
553
554
555
556

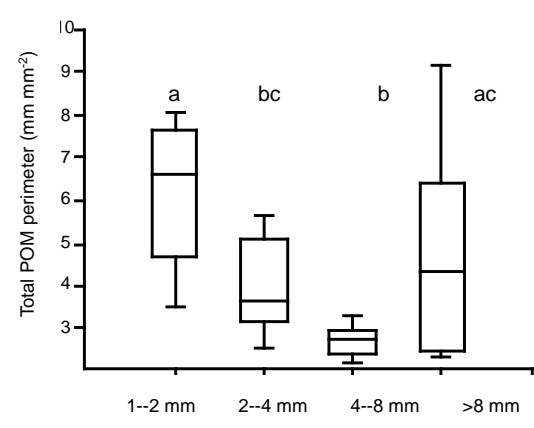
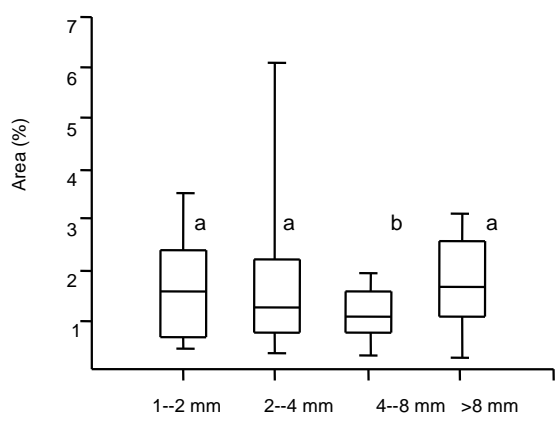
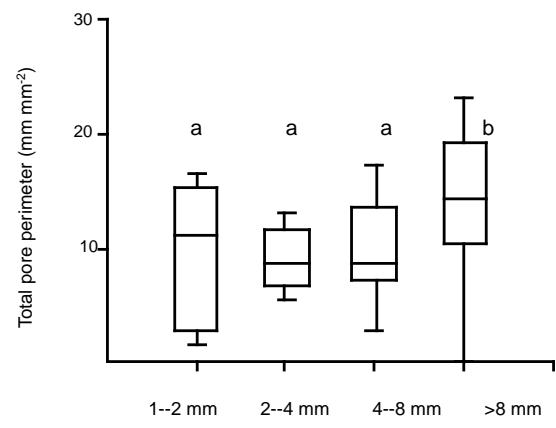
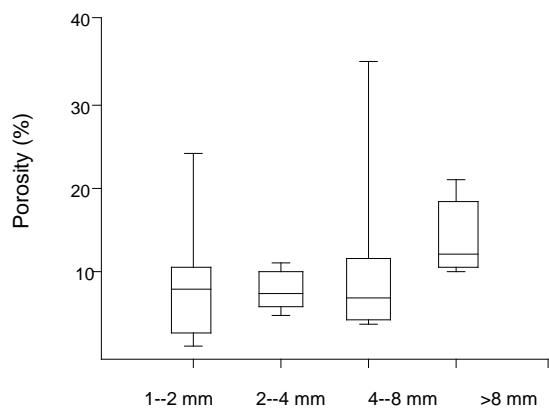
Fig. 3.



557

558 Fig. 4.

559



560
 561
 562 Fig. 5.